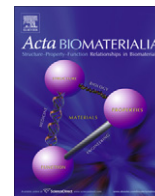




Contents lists available at ScienceDirect

Acta Biomaterialia

journal homepage: www.elsevier.com/locate/actabiomat



Alginate microbeads are complement compatible, in contrast to polycation containing microcapsules, as revealed in a human whole blood model

Anne Mari Rokstad^{a,*}, Ole-Lars Brekke^b, Bjørg Steinkjer^a, Liv Ryan^a, Gabriela Kolláriková^c, Berit L. Strand^d, Gudmund Skjåk-Bræk^d, Igor Lacík^c, Terje Espevik^a, Tom Eirik Mollnes^{e,f}

^a Department of Cancer Research and Molecular Medicine, Norwegian University of Science and Technology, Trondheim, Norway

^b Department of Laboratory Medicine, Nordland Hospital, Bodø and University of Tromsø, Tromsø, Norway

^c Department of Special Polymers and Biopolymers, Polymer Institute of the Slovak Academy of Sciences, Bratislava, Slovakia

^d Department of Biotechnology, Norwegian University of Science and Technology, Trondheim, Norway

^e Institute of Immunology, Oslo University Hospital Rikshospitalet and University of Oslo, Oslo, Norway

^f Research Laboratory, Nordland Hospital, Bodø and University of Tromsø, Tromsø, Norway

ARTICLE INFO

Article history:

Received 5 November 2010
Received in revised form 17 February 2011
Accepted 9 March 2011
Available online xxx

Keywords:

Alginate
Microcapsule
Microbead
Complement
Biocompatibility

ABSTRACT

Alginate microbeads and microcapsules are presently under evaluation for future cell-based therapy. Defining their inflammatory properties with regard to humans is therefore essential. A lepirudine-based human whole blood model was used as an inflammation predictor by measuring complement and leukocyte stimulation. Alginate microbeads were complement-compatible since they did not activate complement as measured by the soluble terminal complement complex (sTCC), Bb or the anaphylatoxins C3a and C5a. In addition, alginate microbeads were free of surface adherent leukocytes. In contrast, microcapsules containing poly-L-lysine (PLL) induced elevated levels of sTCC, Bb, C3a and C5a, surface active C3 convertase and leukocyte adhesion. The soluble PLL induced elevated levels of sTCC and up-regulated leukocyte CD11b expression. PMCG microcapsules containing poly(methylene-co-guanidine) complexed with sodium alginate and cellulose sulfate triggered a fast sTCC response and C3 deposition. The PMCG microcapsules were still less activating than PLL-containing microcapsules as a function of time. The amounts of anaphylatoxins C3a and C5a were diminished by the PMCG microcapsules, whereas leukocyte adherence demonstrated surface activating properties. We propose the whole blood model as an important tool for measuring bioincompatibility of microcapsules and microbeads for future applications as well as determining the mechanisms leading to inflammatory reactions.

© 2011 Acta Materialia Inc. Published by Elsevier Ltd. All rights reserved.

1. Introduction

Cell-based therapy using alginate containing microspheres has been suggested for the treatment of hormone deficiencies [1] as well as brain cancer [2]. The long-term function in experimental animals is, however, often hampered by overgrowth reactions leading to reduced graft performance [1]. The factors contributing to graft failure of the encapsulated cells are only partly understood. There is currently a need for experimental models relevant to humans reflecting the complexity of host factors that are encountered upon transplantation. Human blood contains most of the cells and effectors of the inflammatory machinery, thus it could be used as a source. The critical steps required to mimic the physiological in vivo situation using whole blood lie in the sampling, anticoagulation and incubation conditions, which need to be fully controlled.

Biomaterials in direct contact with blood induce immediate inflammatory responses through plasma cascades like the complement, coagulation and contact systems, with subsequent interplay with inflammatory cells [3]. The level of activation is closely related to the surface properties of the materials. The activation of complement may thus be a sensitive indicator of the ability of a biomaterial to trigger inflammatory reactions. In the present work we have used the novel whole blood model anti-coagulated with the hirudin analog lepirudin [4] to study different microcapsules containing alginate with a focus on complement and leukocyte activation. Lepirudin specifically inhibits thrombin in the coagulation cascade while not affecting the complement cascade and inflammatory cells [4]. In this way it has been possible to study the mutual interactions between complement and leukocytes, as well as between other branches of the inflammatory network.

Complement is a major pro-inflammatory system that acts upstream of the leukocyte and cytokine responses. The complement system consists of around 30 plasma and membrane-bound proteins. The central event of complement activation is cleavage

* Corresponding author. Tel.: +47 72825353; fax: +47 72571463.
E-mail address: anne.m.rokstad@ntnu.no (A.M. Rokstad).

of the C3 protein into the opsonin C3b and the anaphylatoxin C3a. C3 is cleaved by the C3 convertase from the classical/lectin pathway (C4bC2a) or from the alternative pathway (C3bBb), depending on the activators. The activators on a biomaterial surface may be adsorbed IgG inducing classical activation or various forms of C3b (e.g. conformationally changed C3 [5] and/or spontaneously hydrolyzed C3b analog C3(H₂O)) inducing alternative pathway activation. Irrespective of the initial event leading to C3b deposition, this essential step initiates amplification by the alternative pathway convertase, leading to escalated C3 activation. Surface bound C3b is further assembled with the C3 convertases to form the C5 convertases (C4bC2aC3b and C3bBbC3b), which cleave C5 to C5a and C5b. The anaphylatoxin C5a is the most potent inflammatory mediator of complement, whereas C5b is the staging point for formation of the terminal C5b-9 complement complex (TCC) on cell membranes or in solution, sC5b-9 (sTCC) [6]. The ability of biomaterials to trigger complement activation seems to be directly related to whether C3b is able to form covalent links to the surface hydroxyl or amino groups. This linkage may be formed directly on biomaterial surfaces [7] or through adsorbed proteins exposing hydroxyl or amino groups [8]. In addition, the amount of bound water to the surface polymers might be important for their complement activating abilities [9].

To our knowledge, complement reactions to alginate microbeads (Ca²⁺ and Ba²⁺ crosslinked alginate) and microcapsules (an alginate core with a polycation/polyanion complexed membrane) have not been addressed before. By using the lepirudin-based whole blood model the ability of various types of microspheres to activate complement could be studied under identical conditions. Alginate microbeads [10,11] and PMCG microcapsules [12–14] considered for future pancreatic islet transplantation were evaluated. In addition, poly-L-lysine (PLL) containing microcapsules were included to further elucidate the mechanisms behind their inflammatory reactivity [15–18].

Thus, the aim of the present study was to compare the inflammatory potential of different alginate microspheres, as their ability to activate complement and leukocytes using the human lepirudin anti-coagulated whole blood model.

2. Materials and methods

2.1. Study design

The study included five different types of microspheres: Ca/Ba beads (gelled in 1 mM BaCl₂/50 mM CaCl₂), Ba beads (gelled in 20 mM BaCl₂), APA microcapsules (Ca beads coated with PLL and alginate), AP microcapsules (Ca beads coated with PLL) or PMCG microcapsules, formed by polyelectrolyte complexation between sodium alginate (SA)/cellulose sulfate (CS) with polycation poly(methylene-co-guanidine) hydrochloride (PMCG) and calcium cations. All microspheres were made with ultrapure alginate (specified in Section 2.2). In addition, dissolved UP-MVG was evaluated as the alginate source for the microbeads.

2.2. Reagents and equipments

Ultrapure sodium alginates acquired from FMC BioPolymer AS (NovaMatrix, Sandvika, Norway) were used: Pronova UP-MVG (67% guluronic acid, intrinsic viscosity 1105 ml g⁻¹, endotoxin <43 EU g⁻¹), Pronova UP-LVG (66% guluronic acid, intrinsic viscosity 830 ml g⁻¹, endotoxin <100 EU g⁻¹) or Pronova UP100 M (*Macrocystis pyrifera*, 44% guluronic acid, intrinsic viscosity 908 ml g⁻¹, endotoxin <26 EU g⁻¹). The protein content was less than 0.3% for all alginates, as specified by the manufacturer. Cellulose sulfate (CS) sodium salt was from Acros Organics (Geel, Belgium), PMCG

hydrochloride supplied as a 35% aqueous solution was from Scientific Polymer Products Inc. (Ontario, NY). Sodium chloride, calcium chloride, barium chloride and sodium citrate of analytical grade were from Merck (Darmstadt, Germany). Poly-L-lysine hydrochloride (P2658, lot No. 96H5502), Tween 20, zymosan, phosphate-buffered saline (PBS) with calcium and magnesium, ethylenediaminetetraacetic acid (EDTA), paraformaldehyde and LDS-751 were all purchased from Sigma-Aldrich (St Louis, MO). Other reagents, were mannitol (HPLC degree, BDH Analar, VWR International, Pool, UK), sterile saline (0.9% NaCl), non-pyrogenic (B. Braun, Melsungen, Germany), lepirudin (Celgene Europe, Boudry, Switzerland). Antibodies had the following specifications: fluorescein isothiocyanate (FITC) control antibody (BD555057), anti-CD14 FITC (BD347497) and anti-CD11b phycoerythrin (PE; BD347557), all from Becton Dickinson (San Jose, CA). In addition, FITC-conjugated rabbit anti-human C3c (F0201, Dako, Glostrup, Denmark), FITC-conjugated poly rabbit anti-mouse (F0261, Dako, Glostrup, Denmark), anti-human C5b-9 (clone aE11, Diatec, Oslo, Norway) and biotinylated 9C4 [19] were used. For blood sampling the following equipment was used: Nunc 1.8 and 4.5 ml polypropylene vials (Nunc, Roskilde, Denmark) and a BD vacutainer top (Becton Dickinson, Plymouth, UK).

2.3. Microsphere preparation

2.3.1. Alginate microbeads and microcapsules

Ca/Ba beads and Ba beads as well as APA and AP microcapsules were made as described previously using 1.8% UP-MVG alginate [20]. The gelling solution varied according to the type of microsphere: Ca/Ba beads, 1 mM BaCl₂/50 mM CaCl₂ in 0.15 M mannitol; Ba beads, 20 mM BaCl₂ in 0.15 M mannitol; APA and AP, 50 mM CaCl₂ in 0.15 M mannitol. PLL was used at a concentration of 0.05% and incubation was for 10 min. As the outer coating for the APA microcapsules a solution of 0.1% Pronova UP100 M in 0.15 M mannitol was used. The microspheres were made with sterile solutions and under strictly sterile conditions, using autoclaved equipment and a sterile hood for all steps.

2.3.2. PMCG microcapsules

Before the formation of PMCG microcapsules the polyelectrolytes were prepared as follows. PMCG was isolated by lyophilization, ending with a residual water content of less than 2%. CS was purified by treatment with activated charcoal, filtration and precipitation in acetone as described previously [21]. The residual water content of CS was about 10%.

PMCG microcapsules were prepared as described previously [14], except for the following concentration changes in the polymer solutions. The polyanion solution contained 0.90% UP-LVG, 0.90% CS (taking into account the residual water content) in 0.9% NaCl. The polycation solution contained 1.2% PMCG, 1% CaCl₂, 0.9% NaCl and 0.025% Tween 20. A multi-loop reactor [22] provided a continuous encapsulation process with a reaction time of about 40 s for polyelectrolyte complexation. Equilibration of membrane composition was obtained by treatment with 50 mM sodium citrate in 0.9% NaCl solution, pH 7.4 for 10 min. The additional coating layer was made with 0.1% CS in 0.9% NaCl solution for 10 min.

2.4. Whole blood model

2.4.1. Preparation of microspheres and controls for experiments

It is essential that the proportions by volume between blood and additives are equal in the whole blood experiments. The total volume of each additive was 200 µl. Of this, 100 µl consisted of saline containing either 50 µl microspheres, 900 µg UP-MVG alginate, 10 µg zymosan (positive control) or saline (negative control). The amount of soluble alginate corresponds to the alginate content

200 within 50 µl of microbeads. To these additives was added 100 µl of
201 PBS (with CaCl₂/MgCl₂) immediately before addition of 500 µl of
202 whole blood.

203 2.4.2. Whole blood model performance

204 Single experiments for each blood donor were performed as
205 previous described using lepirudin (50 µg ml⁻¹) as the anticoagu-
206 lant [4]. Blood was withdrawn into low activating polypropylene
207 Nunc tubes (4.5 ml). Immediately thereafter, 500 µl of whole blood
208 were added to the various additives in low activating sterile Nunc
209 tubes (1.8 ml). Avoiding blood contamination of the screw cap is
210 essential to avoid biased activation. The samples were incubated
211 for 30, 120 and 360 min in an incubator (37°C) under continuous
212 rotation. Complement activation was stopped by adding EDTA
213 (10 mM final concentration) and centrifugation (3000 r.p.m.,
214 15 min). Aliquots of plasma were stored at -80 °C before analysis.

215 2.5. C3 deposition

216 After incubation of the microspheres in whole blood (Section
217 2.4) the complement cascade was stopped by addition of EDTA
218 (10 mM final concentration). Microspheres were harvested and
219 washed (3×) in a wash solution (0.1% bovine serum albumin,
220 2 mM CaCl₂, 0.02% sodium azide in saline). For each type of micro-
221 sphere one fraction was added to 50 µg ml⁻¹ FITC-conjugated poly
222 rabbit anti-human C3c (C3 deposition) and the other FITC-conju-
223 gated poly rabbit anti-mouse (control) antibodies. The samples
224 were protected from light and continuously agitated for 30 min.
225 Thereafter the microspheres were washed (3×). The deposition of
226 C3 was visualized by confocal laser scanning microscopy (CLSM)
227 (Zeiss LSM 510, Carl Zeiss MicroImaging GmbH, Göttingen, Ger-
228 many) with a 488 nm laser source (BP 505–530). Identical laser
229 settings were used on all microspheres using PMCG and APA
230 microcapsules incubated for 120 min as references.

231 2.6. Expression of CD11b

232 Expression of CD11b was measured after 15 min incubation in
233 whole blood as described in Section 2.4. Whole blood was fixed
234 with 0.5% PFA in an equal volume for 4 min at 37 °C, and then
235 stained with PE anti-CD11b, FITC anti-CD14 and the nuclear dye
236 LDS-751 and analyzed using a flow cytometer (Beckman Coulter
237 Epics XL-MCL, Coulter Corp, FL). To exclude red cells and debris
238 the threshold was set at FL-3. Granulocytes and monocytes were
239 gated in a SSC/FITC anti-CD14 dot plot, and CD11b expression mea-
240 sured as mean fluorescence intensity (MFI).

241 2.7. Cell adherence

242 Microspheres were prepared as described in Section 2.4 and
243 incubated for 180 min. Blood was removed and the microspheres
244 fixed in 0.5% PFA for 20 min. In order to keep the cells attached
245 the blood samples were prepared without addition of EDTA, as
246 would otherwise have been used to stop the complement cascade.
247 From each sample one fraction was stained with antibodies
248 (7.5 µg ml⁻¹ in PBS) against CD14 (FITC anti-CD14) and CD11b
249 (PE anti-CD11b) or with control antibodies (FITC mouse IgG2b,κ/
250 PE mouse IgG2a,κ). Both combinations were incubated for
251 30 min in the dark and under continuous agitation, thereafter care-
252 fully washed and finally 0.15% PFA was added. Evaluation of the
253 microspheres was performed using CLSM (Zeiss LSM 510, Carl Zeiss
254 MicroImaging GmbH, Göttingen, Germany), with 488 nm (BP 505–
255 530) and 543 nm (LP 650) excitation and emission wavelengths,
256 respectively.

257 2.8. Assay of complement activation

258 2.8.1. sTCC

259 The terminal sC5b-9 complex (sTCC) was quantified by electro-
260 immunoassay using mAb aE11 specific for C9 incorporated in the
261 sC5b-9 complex and biotinylated 9C4 specific for C6 in the respec-
262 tive complex. The assay has been described in detail previously [6]
263 and was performed according to a later modification [19].

264 2.8.2. Bb, C3a and C5a

265 C3a and Bb was analyzed by ELISA using kits from Quidel (San
266 Diego, CA). C5a was analyzed using an ELISA kit from BD Bioscience
267 (San Diego, CA).

268 2.9. Statistical methods

269 One-way repeated measurements ANOVA with Dunnet's multi-
270 ple comparison test were used to define statistical differences be-
271 tween saline and the other additives at a given time point.
272 Differences for the various additives over time were tested using
273 a two-way ANOVA. The data was not normally distributed due to
274 the low sample numbers (n = 5), therefore the data were log trans-
275 formed before analysis. Differences were considered significant at
276 P < 0.05.

277 2.10. Ethics

278 The use of human whole blood for basal experiments was ap-
279 proved by the Regional Ethic Committee at the Norwegian Univer-
280 sity of Science and Technology. The experiments were performed
281 in accordance with their guidelines.

282 3. Results

283 3.1. Activation of the complement cascade detected as sTCC formation
284 in human whole blood

285 The formation of sTCC indicates activation of the complement
286 cascade and is suggested to be the most sensitive and specific mar-
287 ker of complement activation. Fig. 1A shows the time kinetics of
288 sTCC formation after addition of saline, Ca/Ba beads and APA and
289 PMCG microcapsules as well as zymosan. The kinetics of sTCC acti-
290 vation were significantly different (P < 0.0001) for each additive.
291 Fig. 1B–D shows the data for the entire panel of additives at each
292 time point. After 30 min incubation the amount of sTCC was simi-
293 lar for the Ca/Ba beads, Ba beads and saline control (Fig. 1B). Over
294 time, the generation of sTCC was slower for Ca/Ba beads and Ba
295 beads compared with the saline control (Fig. 1C and D). This re-
296 sulted in significantly lower values (P < 0.05) for Ba beads after
297 120 and 360 min incubation and for Ca/Ba beads after 360 min
298 (Fig. 1D). The polycation containing microcapsules, APA, AP and
299 PMCG, resulted in significant increases (P < 0.05) in sTCC compared
300 with saline at all time points (Fig. 1B–D). The APA and AP micro-
301 capsules showed a time-dependent increase in sTCC (Fig. 1B–D).
302 The PMCG microcapsules induced a rapid initial increase in sTCC,
303 detected after 30 min (Fig. 1B). This was followed by a slower in-
304 crease compared with the APA and AP microcapsules at 120
305 (Fig. 1C) and 360 min (Fig. 1D). The dissolved UP-MVG alginate
306 induced a small increase in sTCC after 30 min, although non-signif-
307 icant (Fig. 1B). After 120 and 360 min the sTCC amounts where
308 slightly lower than for the saline control (Fig. 1C and D). The
309 amount of UP-MVG alginate (900 µg) corresponded to the amount
310 of alginate in the aliquots of microbeads. The data therefore
311 indicate minor differences between dissolved and gelled alginate.

3.2. Alternative pathway factor B activation

The amount of Bb, an activation product of the alternative pathway factor B, increased with time (Fig. 2A–D) in a pattern resembling the sTCC data. The increase in Bb was, however, slower compared with sTCC. The kinetics of Bb formation were significantly affected ($P < 0.0001$) by each additive (Fig. 2A). In samples containing Ca/Ba beads, Ba beads or dissolved UP-MVG alginate the amounts of Bb were lower than for the saline control over time (Fig. 2C and D), with a significant ($P < 0.05$) difference at 360 min (Fig. 2D). The highest concentration of Bb was found in samples containing APA and AP microcapsules. The increase was significant for AP at 120 and 360 min (Fig. 2C), and for APA at 360 min (Fig. 2D). A non-significant elevation of Bb was found in the samples incubated with PMCG microcapsules for 30 min (Fig. 2B). The early induction at 30 min was followed by an evident and significant ($P < 0.05$) increase after 120 min (Fig. 2C). Interestingly, the amount of Bb was not further increased by the PMCG microcapsules at 360 min (Fig. 2D). The saline control, however, showed a steady increase, which resulted in similar Bb amounts for the PMCG microcapsules and saline control after 360 min (Fig. 2D).

3.3. Anaphylatoxin C3a and C5a release

The anaphylatoxins C3a and C5a are potent pro-inflammatory molecules derived from the cleavage of C3 and C5. The kinetics of C3a production are shown in Fig. 3A after addition of Ca/Ba beads and APA and PMCG microcapsules and for the controls. The kinetics were significantly different ($P < 0.0001$) for each additive (Fig. 3A). At the specific time points only a few of the additives resulted in significantly different C3a amounts relative to the saline control. The trends in stimulation were still consistent with the sTCC and Bb findings, with the exception of the PMCG microcapsules. Briefly, addition of Ca/Ba beads and Ba beads resulted in lower concentrations of C3a after 120 and 360 min (Fig. 3C and D), while addition of APA and AP microcapsules increased C3a (Fig. 3B–D). The PMCG microcapsules initially gave a slight elevation of C3a (Fig. 3B). However, after 120 and 360 min the PMCG microcapsules resulted in significantly ($P < 0.05$) lower amounts of C3a than saline (Fig. 3A–D). The dissolved UP-MVG alginate induced a slight but significant ($P < 0.05$) increase in C3a after 30 min (Fig. 3B), but after 120 and 360 min the amount of C3a was lower than for the saline control (Fig. 3C and D). A particular finding for the saline solution was the pronounced increase in C3a over time. This may be due to activation by the plastic surface [23].

The kinetics of C5a production were also significantly different ($P < 0.0001$) in response to Ca/Ba beads and APA and PMCG microcapsules and the controls (Fig. 4A). After 30 min Ca/Ba beads and Ba beads resulted in non-significant, slight increases in C5a levels relative to the saline control (Fig. 4B). The C5a increase was slower for Ca/Ba beads and Ba beads (Fig. 4C and D) compared with saline, resulting in significantly ($P < 0.05$) lower amounts after 360 min (Fig. 4D). A rise in C5a was detected on addition of APA and AP microcapsules, giving significant increases ($P < 0.05$) for APA at all time points and for AP at 120 and 360 min (Fig. 4B–D). PMCG microcapsules initially gave a modest, but statistically significant ($P < 0.05$), increase in C5a (Fig. 4B). Over time the PMCG microcapsules resulted in lower C5a amounts compared with the saline control, with a significant ($P < 0.05$) difference after 360 min (Fig. 4D).

3.4. C3 deposition on the microsphere surface

Deposition of C3 on the different microsphere surfaces is shown in Fig. 5. The detected C3c fragment of the C3 molecule

is present in both the native C3 molecule, the active C3b convertase and its analog C3(H₂O). Detected C3 may, therefore, represent either adsorbed native C3 molecule or the active C3 convertase (C3b or the analog C3(H₂O)) on the microsphere surface. The deposition of C3 on the surface of Ca/Ba beads and APA, AP and PMCG microcapsules is shown at different incubation times (Fig. 5A–L). After 30 min a slight C3 staining was detected for Ca/Ba beads (Fig. 5A) and APA (Fig. 5B) and AP microcapsules (Fig. 5C). In contrast, the PMCG microcapsules showed pronounced staining at 30 min (Fig. 5D). The C3 staining on the PMCG microcapsules revealed surface irregularities and ruptures (Fig. 5D). No further increase in C3 staining was observed for the PMCG microcapsules after 120 (Fig. 5H) and 360 min (Fig. 5L). The surfaces of the APA (Fig. 5F and J) and AP microcapsules (Fig. 5G and K) showed increased staining with time. C3 staining also increased with time for the Ca/Ba beads (Fig. 5E and I). However, Ca/Ba beads with low detectable staining were estimated to form approximately 70–90% of the microbead population at all time points. The C3 distribution pattern was smooth and evenly distributed on the Ca/Ba beads (Fig. 5E and I). For the APA (Fig. 5B, F and J) and AP (Fig. 5C, G and K) microcapsules, C3 accumulated at certain points, resulting in spotted patterns. Further, equatorial sections of the microspheres at 360 min showed C3 located on the surface of the microspheres (Fig. 5M–P). The depth of penetration of C3 was estimated by LSM510 software fluorescence intensity profile analysis, as shown in Fig. A1. This analysis indicated that the Ca/Ba beads were most permeable, since C3 was found to penetrate 10–125 μm into the microbeads (S1A–B). Shorter penetration depths was found for the microcapsules, estimated at 20–40 μm for APA (Fig. A1C and D), 10–20 μm for AP (Fig. A1E and F) and 20 μm for the PMCG microcapsules (Fig. A1G and H). The staining was specific for C3, as demonstrated by the negative controls with corresponding insets showing light transmission (Fig. 5Q–T).

3.5. Leukocyte activation as measured by CD11b expression and cell adherence to the different microspheres

CD11b is the receptor for iC3b and an early activation marker of leukocytes. Granulocyte and monocyte CD11b expression was analyzed by flow cytometry 15 min after addition of microspheres or controls (Fig. 6A and B). The PMCG microcapsules showed significantly ($P < 0.05$) higher granulocyte CD11b expression compared with the saline control (Fig. 6A). CD11b expression was also higher on monocytes, although not statistically significantly so (Fig. 6B). The APA and AP microcapsules also resulted in a slight increase in granulocyte CD11b, although not significantly (Fig. 6A). An overall, moderate increase in CD11b expression was found on addition of the different microcapsules compared with yeast zymosan.

Leukocyte adherence on microspheres was evaluated after incubation in whole blood for 3 h (Fig. 6C–J). Leukocytes did not adhere to the Ca/Ba beads (Fig. 6C) or Ba beads (Fig. 6D). However, adherent leukocytes were found on the surface of APA (Fig. 6E and F), AP (Fig. 6G and H) and PMCG microcapsules (Fig. 6I and J). Cells appeared as small circular dots on the surface of the microcapsules and in the surrounding area, as seen by transmitted light (Fig. 6F, H and J). The larger fraction of the adherent cells stained positive for CD11b, while a smaller fraction stained positive for CD14 (Fig. 6E, G and I). CD11b is present on both granulocytes and monocytes in only slightly different amounts, while CD14 is expressed in higher amounts on monocytes. The monocytes in the present study displayed 23–50 times higher CD14 expression compared with the granulocytic population (data not shown). This indicates that the adherent cells were mainly granulocytes, with fewer numbers of monocytes.

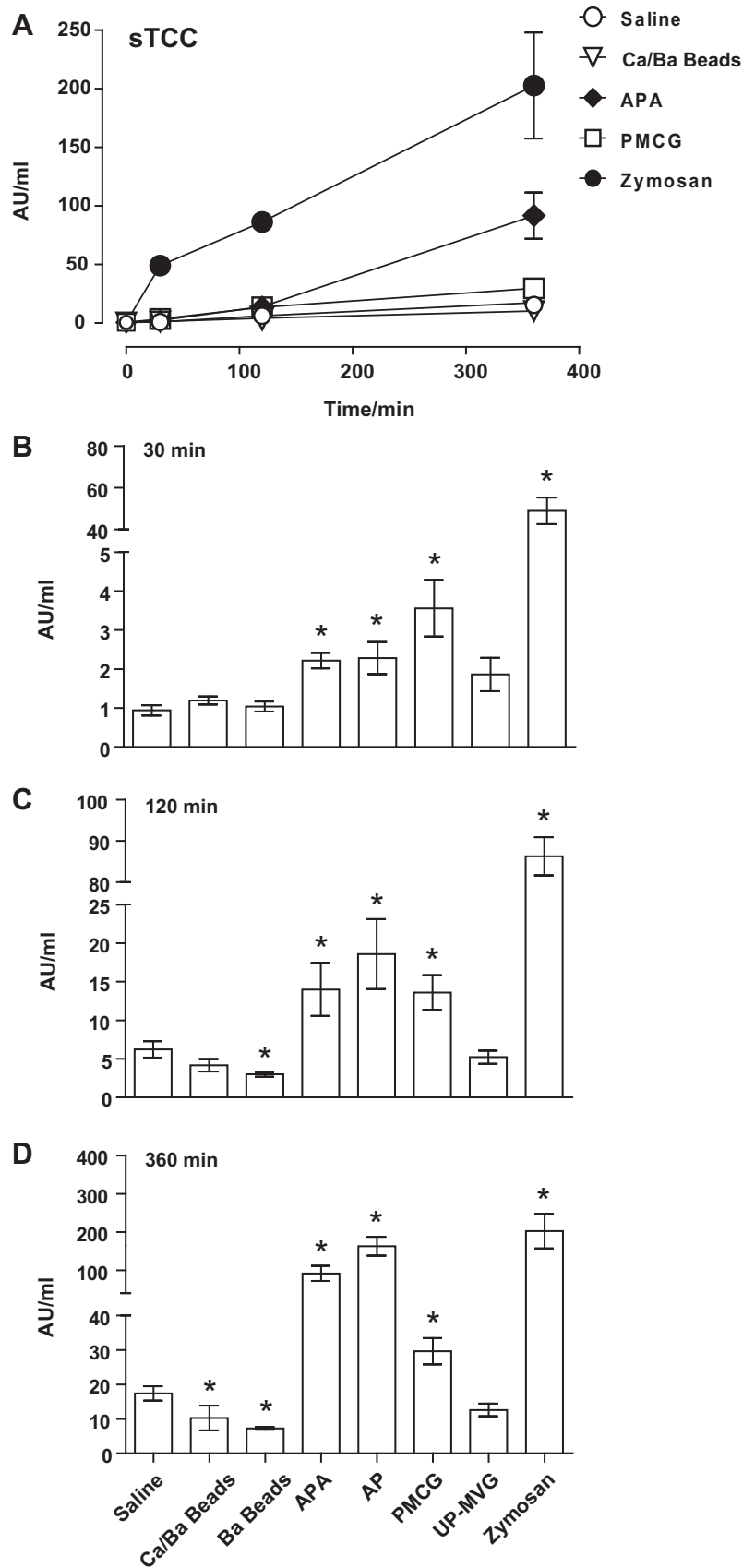


Fig. 1. sTCC concentration in plasma after incubation with various microspheres, alginate and controls in human lepirudin anti-coagulated whole blood. (A) Time-dependent sTCC amounts after addition of Ca/Ba Beads, APA, PMCG microcapsules, saline and zymosan. The additives significantly ($P < 0.0001$) affect sTCC formation over time. In the lower three panels each time point is shown (B) 30, (C) 120 and (D) 360 min with additional Ba beads, AP microcapsules and dissolved UP-MVG alginate included. (B–D) $*P < 0.05$. The baseline sTCC value measured in the sample at the start of the experiment was $0.55 \pm 0.16 \text{ AU ml}^{-1}$. Data are expressed as means \pm SEM, $n = 5$.

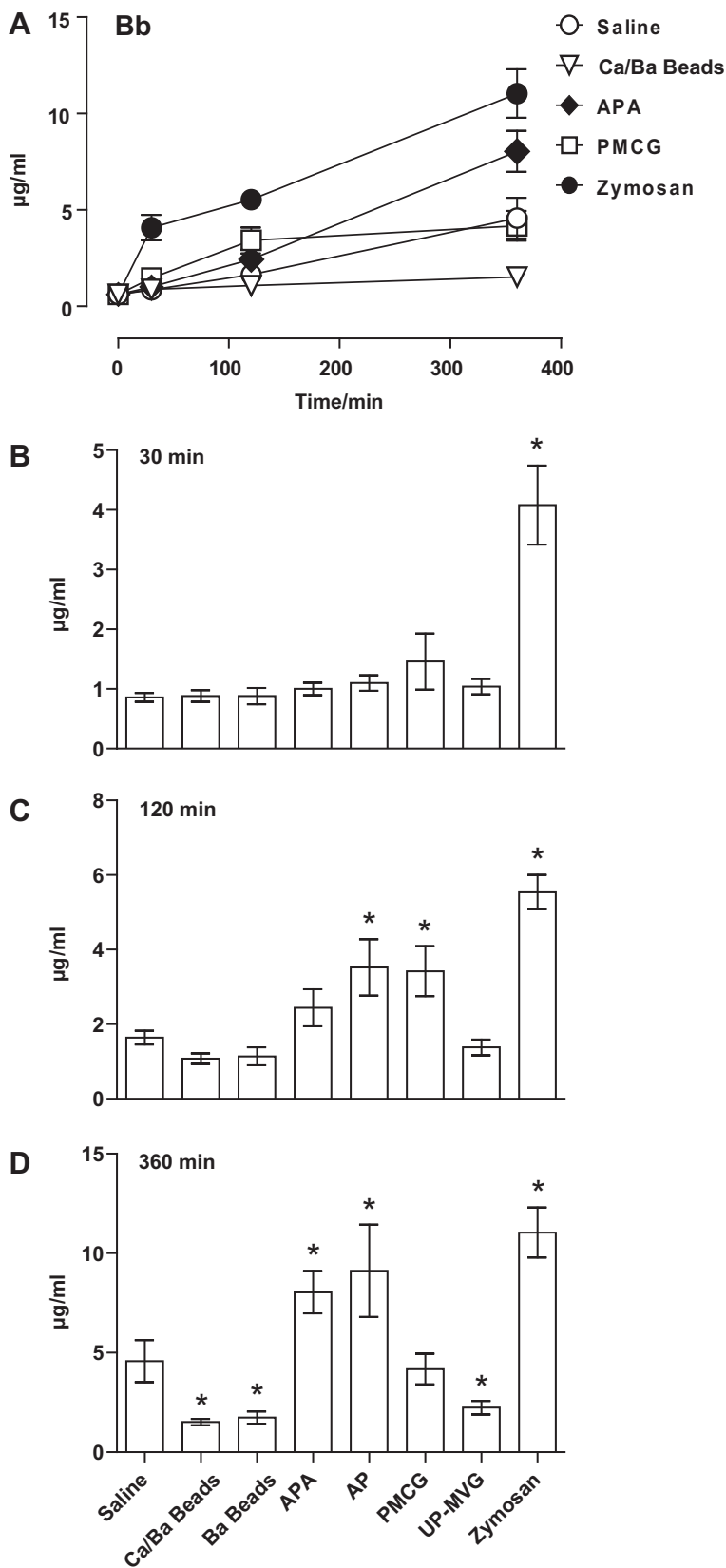


Fig. 2. Bb concentration in plasma after incubation with various microspheres, alginate or controls. The various additives and time parameters in (A)–(D) are as described in Fig. 1. The time-dependent Bb concentration was significantly ($P < 0.0001$) affected by each additive. (B–D) $*P < 0.05$. The baseline value of Bb was $0.62 \pm 0.12 \mu\text{g ml}^{-1}$. Data are expressed as means \pm SEM, $n = 5$.

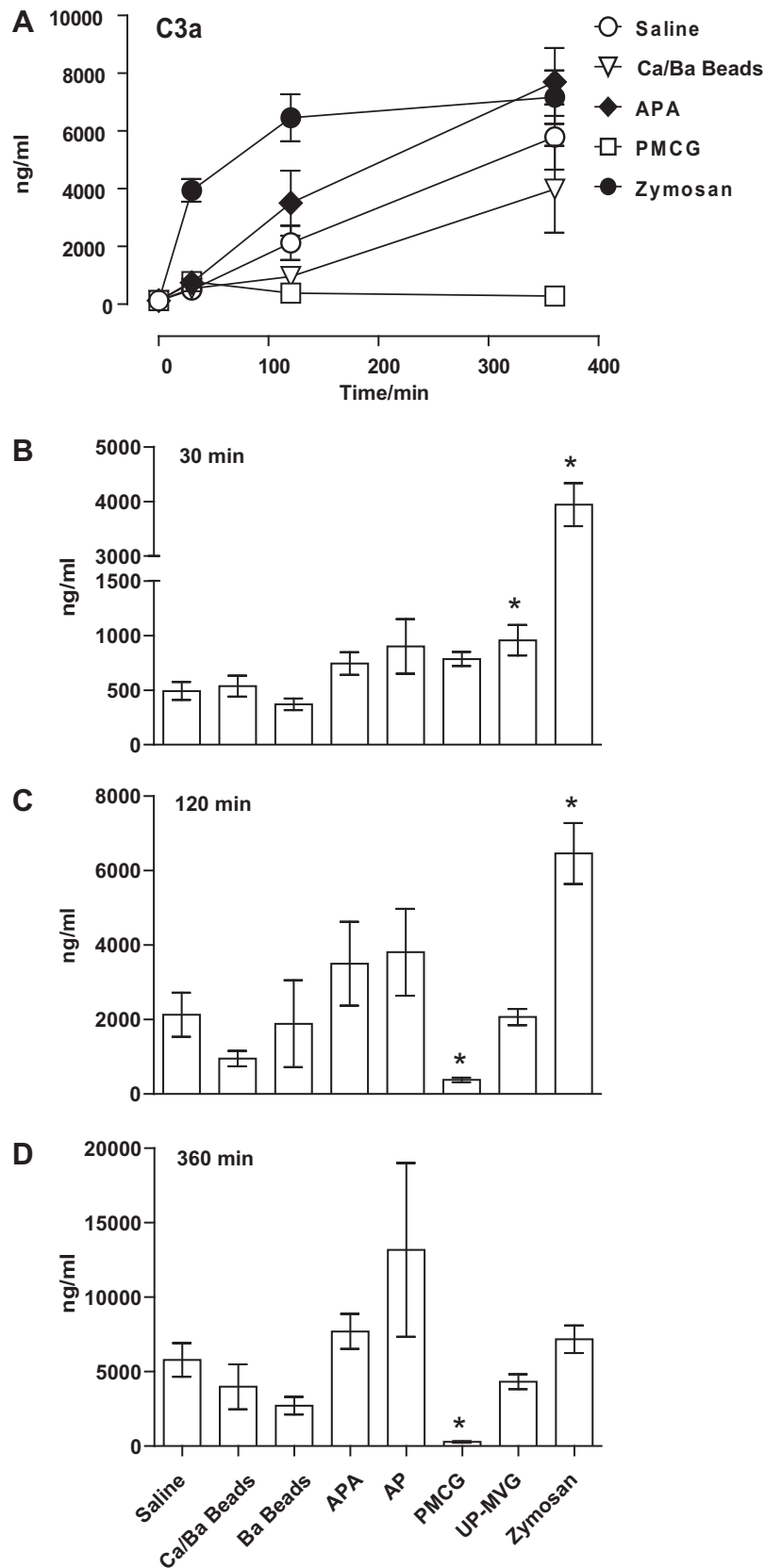


Fig. 3. C3a concentration in plasma after incubation with various microspheres, alginate or controls. The various additives and time parameters in (A)–(D) are as described in Fig. 1. The time-dependent C3a concentration was significantly ($P < 0.0001$) affected by the additives. (B–D) $*P < 0.05$. The baseline value of C3a was $120 \pm 28.8 \text{ ng ml}^{-1}$. Data are expressed as means \pm SEM, $n = 5$.

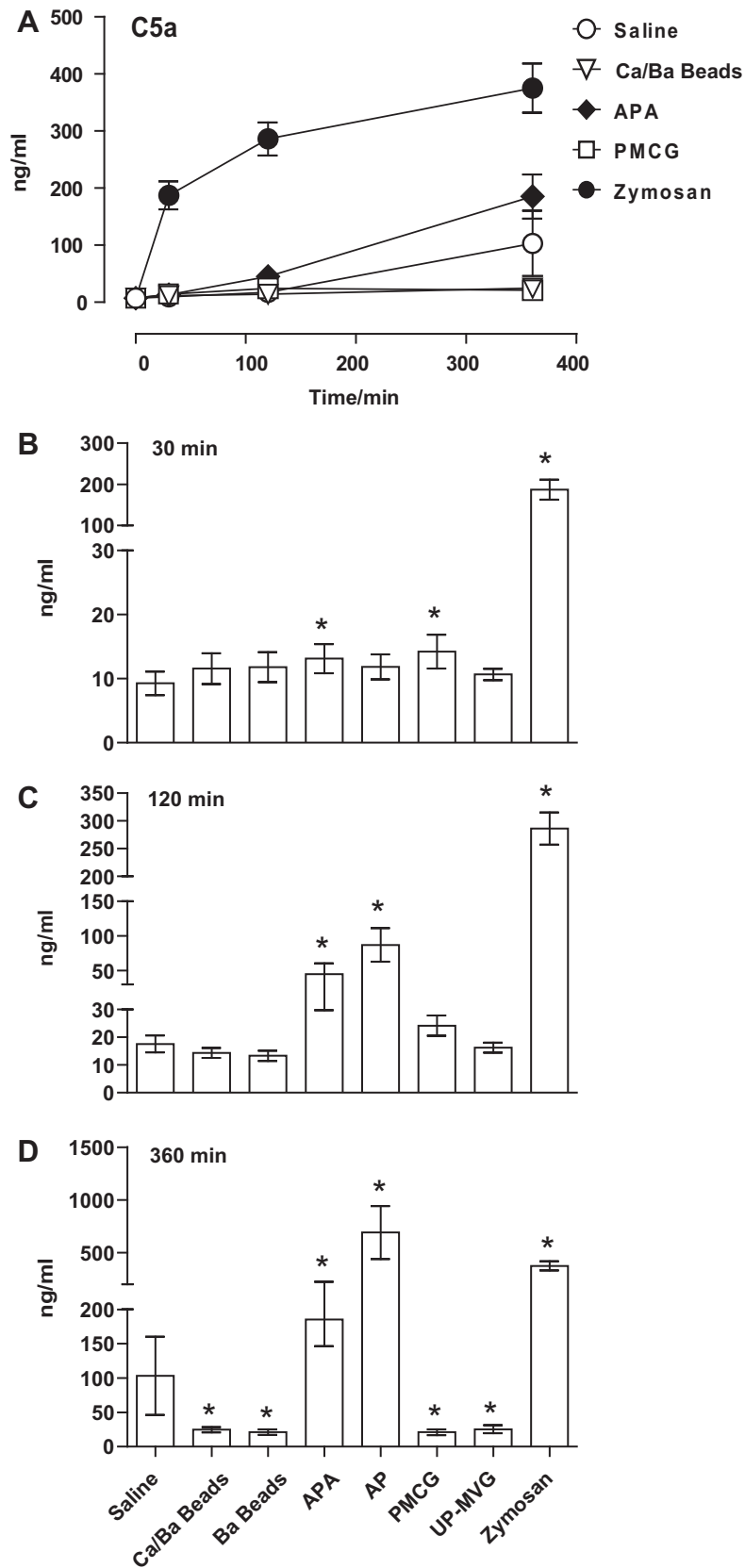


Fig. 4. C5a concentration in plasma after incubation with various microspheres, alginate or controls. The various additives and time parameters in (A)–(D) are as described in Fig. 1. The time-dependent C5a concentration was significantly ($P < 0.0001$) affected by the additives. (B–D) $*P < 0.05$. The baseline value for C5a was $7.27 \pm 0.99 \text{ ng ml}^{-1}$. Data are expressed as means \pm SEM, $n = 5$.

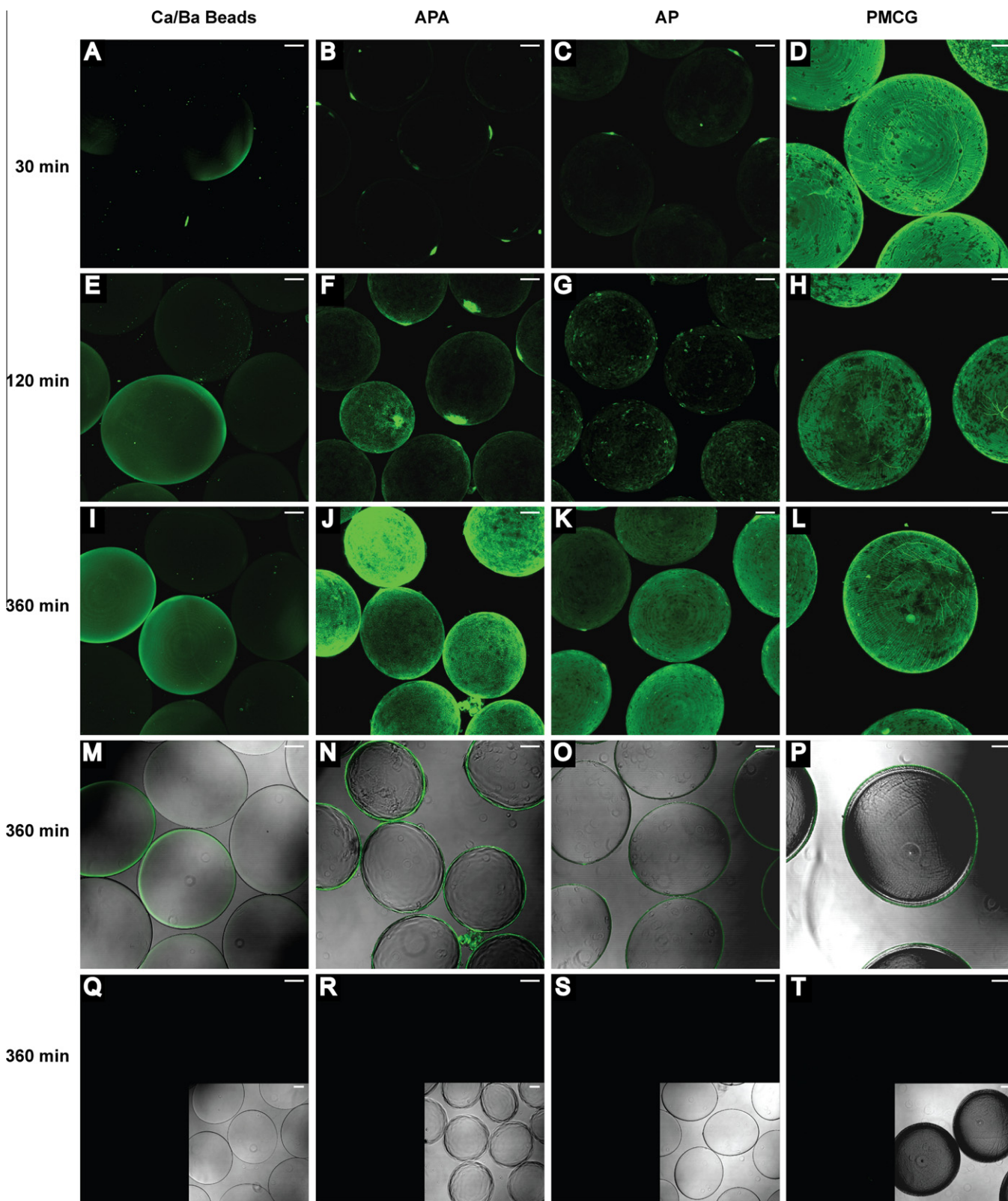


Fig. 5. Deposition of C3 on the microsphere surface after incubation in human lepirudin anti-coagulated whole blood. (A–L) 3D projections made by sectioning entire microspheres after incubation for 30, 120 and 360 min. (M–P) Projections through the equator overlaid with transmitted light images after 360 min. (Q–T) Controls are given in the lower panels as projections (black pictures). The inserts show transmitted light equatorial sections for visualization. Bars are 100 μ m.

437 3.6. Effect of soluble PLL, CS and PMCG

438 The activation potential of dissolved PLL, CS and PMCG was
439 evaluated by measuring sTCC production and CD11b expression.

A clear dose-dependent induction of sTCC was found by addition
of PLL (Fig. 7A). The polycation PMCG resulted in increased sTCC
formation at the highest dose (1000 μ g ml⁻¹), whereas addition
of CS showed a weak inhibitory effect (Fig. 7A). In contrast, CS gave

440
441
442
443

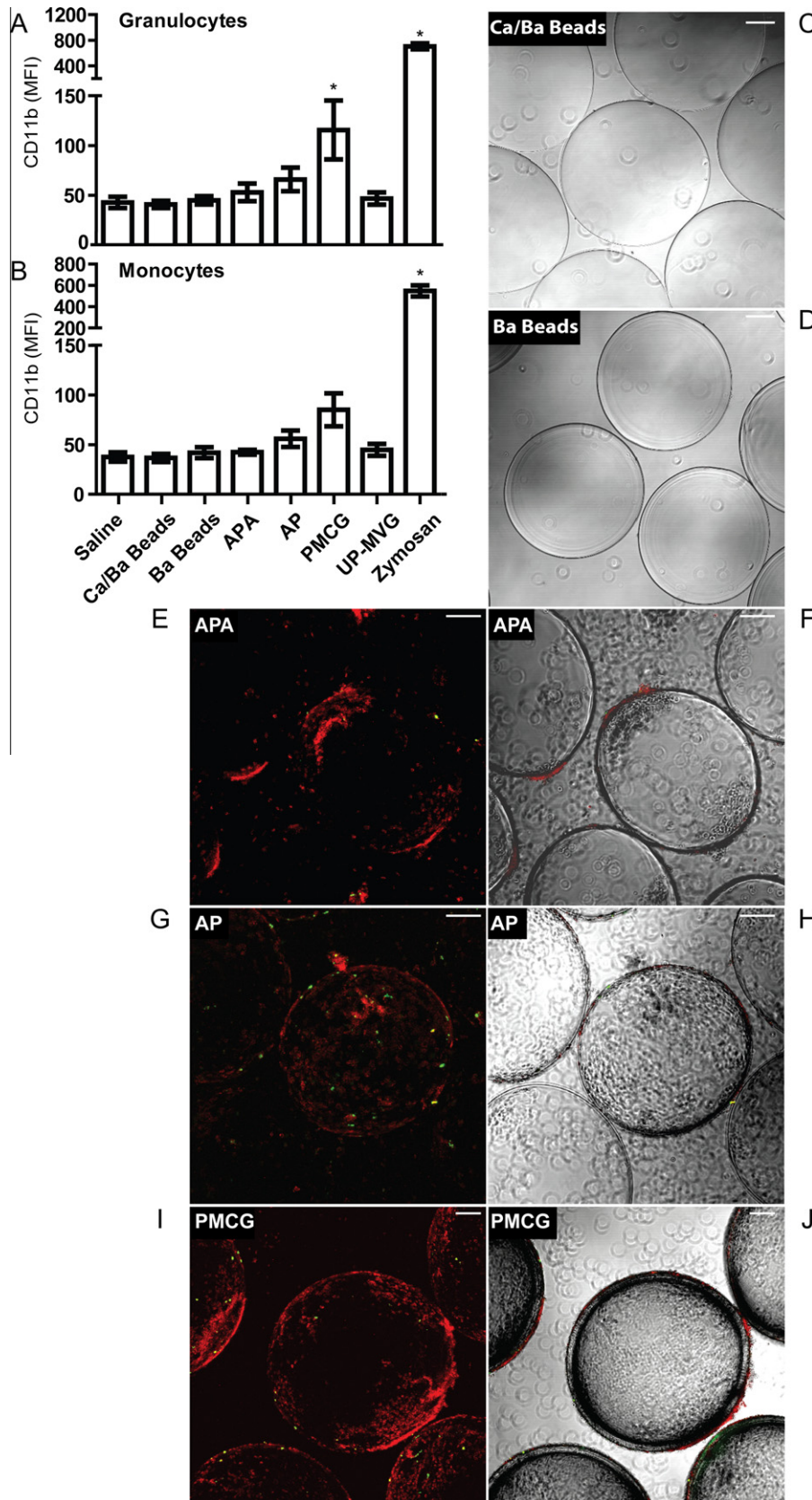


Fig. 6. Leukocyte CD11b expression and surface adhesion after the addition of various microspheres to lepirudin anti-coagulated whole blood. Leukocyte CD11b expression detected by flow cytometry 15 min after addition of microspheres, UP-MVG alginate and controls. (A) Granulocytes CD11b expression and (B) monocytes CD11b expression. Results are given as means \pm SEM, $n = 5$. $*P < 0.05$. (C–J) Leukocyte adhesion on microspheres after 3 h incubation. Images taken by CLSM are presented as optical sections at the equator and 3D projections were produced from several sections through the microspheres. (C) Ca/Ba beads section, (D) Ba beads section, (E) APA projection, (F) APA section, (G) AP projection, (H) AP section, (I) PMCG projection, (J) PMCG section. CD11b is shown in red and CD14 in green. Bars are 100 μ m.

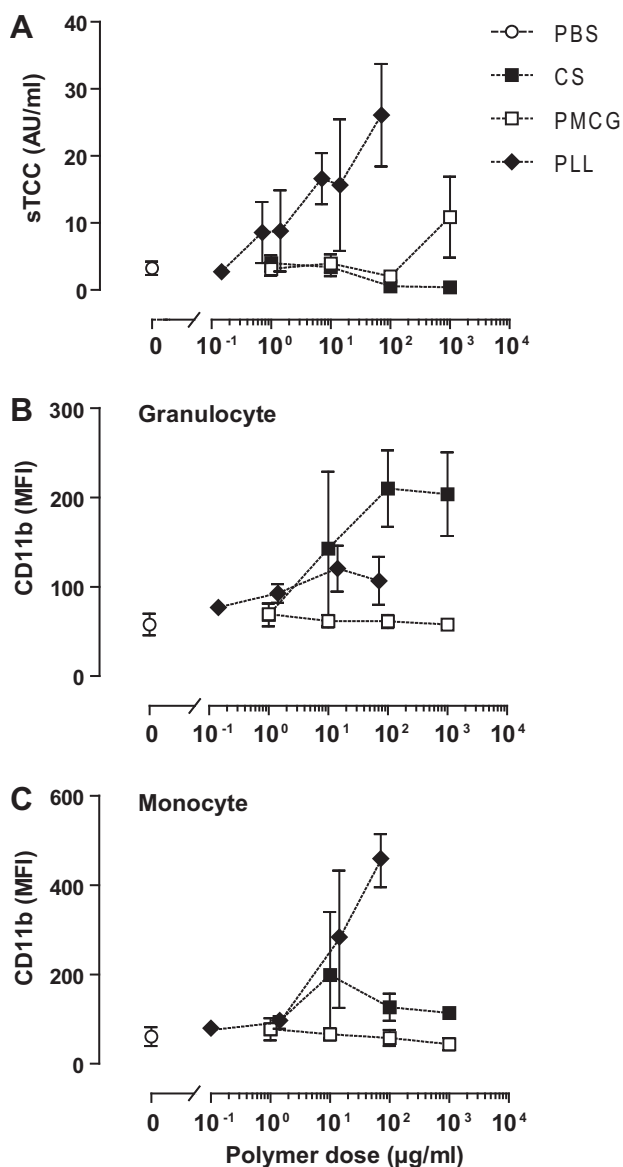


Fig. 7. sTCC concentrations and leukocyte CD11b expression after addition of PLL, CS and PMCG in solution to lepirudin anti-coagulated human whole blood. (A) sTCC after 120 min incubation, (B) granulocyte CD11b expression 15 min after addition, (C) monocyte CD11b expression 15 min after addition. Data are given as mean \pm SEM, $n = 3$ for sTCC and $n = 2$ for CD11b expression.

a clear dose-dependent elevation of CD11b expression in granulocytes (Fig. 7B). Increased granulocyte CD11b expression was also found after addition of PLL (Fig. 7B), although with lower potency than CS. In contrast, dissolved PMCG showed a slight dose-dependent reduction in CD11b expression in both granulocytes (Fig. 7B) and monocytes (Fig. 7C). PLL was a more potent inducer of CD11b expression than CS in monocytes (Fig. 7C). It is important to stress the time difference between the sTCC data from 120 min incubation and the CD11b expression data measured after 15 min incubation.

4. Discussion

The ability of different types of microspheres to provoke complement and leukocyte activation was evaluated using a whole blood model. The whole blood model made it possible to unmask differences in complement and leukocyte activation between the

various types of microspheres. The three types of microcapsules containing polycations activated complement, while the two types of alginate microbeads did not induce activation. The activation was mainly through the alternative pathway, as the patterns of product Bb specific for this pathway corresponded well with the end product sTCC. Also, the level of C4d, formed by activation of the classical or lectin pathway, remained low (data not shown), confirming that activation occurred mainly through the alternative pathway.

The low complement activation from the alginate microbeads suggests a high degree of complement biocompatibility. The slow increase in complement activation in the saline control is consistent with activation of complement induced by the surface of the polypropylene vials used. The lower formation of complement activation products over time by alginate microbeads shows that they are less activating than the polypropylene vials and clearly supports their low activation property. The lower activity of the alginate microbeads compared with the control could be explained by absorption of complement components in the open structured gel matrix, as these alginate microbeads are estimated to be permeable for IgG (150 kDa) [24] and proteins of up to 350 kDa [11]. The C3 protein in its native form has a molecular weight of 185 kDa, thus it should be able to diffuse into the alginate matrix. Penetration of C3 was found in the alginate microbeads to variable depths of 10–125 μm (Fig. A1). Despite this absorption, we emphasize that accessible amounts of C3 should be available for formation of C3 convertase since C3 is abundant in plasma (0.7–1.8 g l⁻¹).

It is suggested that the ability of materials to bind proteins and to induce conformational changes in the proteins is essential for their complement activating capability [8]. Alginate is rich in carboxylic groups, thus negatively charged plasma proteins such as albumin (PI 4.7–5.1), C3 (PI 5.75) and C5 (PI 4.10) will have low affinities for the alginate matrix. C3 will, upon binding to the surface and undergoing a conformational change, expose highly reactive thioester [25] groups, leading to an amplification loop of the alternative pathway [5]. From the present study we could not verify whether the deposited C3 was in its native C3 form or in one of its activated or inactivated forms, as the anti-C3c antibody detects any part of C3 containing the C3c fragment. However, given the low sTCC and Bb concentrations found after incubation with alginate microbeads we suggest that this staining is mainly due to C3 present in its native form, absorbed in the permeable alginate matrix. This is also deduced from the smooth distribution pattern that indicates freely diffusive molecules rather than a process involving active convertases (discussed below). The low complement activation property of the alginate microbeads was also confirmed by a lack of adherent leukocytes, which is consistent with complement being the most likely candidate for leukocyte activation in this model.

In contrast to the alginate microbeads, the APA and AP microcapsules induced elevated levels of sTCC, Bb and anaphylatoxins C3a and C5a (Figs. 1–4), collectively demonstrating substantial complement activation. The anaphylatoxins C3a and C5a are potent inflammatory mediators which may play an active role in the initiation of inflammatory reactions against the APA microcapsules. The present data also demonstrate deposition of C3 fragments on the APA surface, starting as local spots and increasing with time, with prominent deposition after 360 min (Fig. 5). While the detected C3c fragment is present in both native C3 and active C3b, the present data indicate active C3b on the APA surface since: (1) deposition started at specific points giving a spotted pattern, indicating activation loop formation of active convertases; (2) elevated levels of C3a, which is produced in equimolar amounts to activated C3b, were found; (3) elevated levels of C5a indicated C5 convertase formation on the capsule membrane; (4) elevated levels of sTCC indicated formation of active convertases.

Complement activation is shown to be initiated when C3b forms amide bonds with exposed amino groups [7]. Amino groups are abundant within the polypeptide PLL and are likely candidates for C3b surface binding. Soluble PLL also induced an increase in sTCC, demonstrating the complement stimulatory property of PLL.

Ideally the PLL should be neutralized by alginate, as previously demonstrated for soluble polyelectrolytes [17]. However, in APA microcapsules PLL and alginate interact at the surface [20] and PLL is found in relatively high amounts within the 100 Å thick outermost layer of [26]. Although the complex of alginate and PLL has been shown to be evenly distributed in the outermost surface, the degree of interaction may vary, resulting in exposure of PLL in a stimulatory state [26]. Insufficient neutralization of PLL could therefore explain both the stimulatory properties of PLL present in the APA microcapsules as well as the small difference between the AP and APA microcapsules in the present study.

Surface bound iC3b is an important ligand for CD11b/CD18 (CR3 receptor) on leukocytes [27]. CD11b positive cells were found to attach to the surface of APA microcapsules, thus iC3b may have been involved in the observed cell attachment. However, we cannot exclude involvement of other ligands, including surface bound fibrinogen, since this is also a known ligand for the CD11b receptor [28]. The adherent cells on APA microcapsules were mainly granulocytes with a scattered distribution of monocytes. These findings are consistent with normal inflammatory reactions, the early stages of which are dominated by neutrophilic granulocytes. The anaphylatoxin C5a up-regulates neutrophil CD11b expression [29] and may thus contribute to the observed cell attachment.

The PMCG microcapsules initiated the fastest complement activation, as reflected in the early detectable levels of sTCC and Bb and deposition of C3. In combination with the sTCC data this may reflect active convertase formation. However, no further increase in C3 staining was seen after 30 min incubation, indicating reduced convertase formation with time. This was also reflected in the sTCC response, which only doubled between 120 and 360 min incubation, while the APA microcapsules induced an increase of 6–10-fold over the same time period. The explanation for these differences may be found in the ability of the various polyelectrolytes to stimulate or inhibit complement activity, affect surface properties and their ability to form stable complexes. When forming PMCG microcapsules poly(methylene-co-guanidine) diffuses into the CS/alginate microbead and complexes predominantly with CS. Leakage of polyelectrolytes may occur as a result of loose complexation or excess polymer. In the present study PMCG in solution was found to induce an increase in sTCC. Moreover, the soluble CS induced rapid up-regulation of leukocyte CD11b. Thus, rapid activation by the PMCG microcapsules might be explained by the release of polymer, with CS a likely candidate for early leukocyte CD11b up-regulation and PMCG for rapid complement activation. In contrast, soluble CS gave a slight concentration-dependent decrease in sTCC response compared with the control. This finding points towards the reported complement inhibiting activity of cellulose sulfate [30–32] and may thus explain the lower complement stimulatory abilities of the PMCG microcapsules with time.

A particularly interesting finding with the PMCG microcapsules was the low amounts of the anaphylatoxins C3a and C5a detected after the longer incubation times. The increased amount of Bb and particularly sTCC indicates that the anaphylatoxins had been formed. The most plausible explanation is therefore adsorption of the highly positively charged C3a (PI 9.7) and C5a (PI 8.6) to the negatively charged CS on the surface of PMCG microcapsules. This implies that the fluid phase concentrations do not necessarily reflect the activation potential of a surface. Anaphylatoxins present on the surface may still be biologically active and contribute to the leukocyte adherence on the PMCG microcapsule, in addition to the opsonic effect of bound iC3b, as previously discussed.

The complement activation profiles of alginate microbeads and APA microcapsules in the present study correspond well with previous biocompatibility studies showing polycation containing microcapsules to be less biocompatible [15–18,33,34]. In such studies bioincompatibility has been measured as overgrowth reactions that might have been caused by inflammatory reactions. The complement system is a primary inductor of inflammation were its protein effectors reacts upstream of leukocytes and cytokines [4,23,35–37]. Complement activity may therefore be a useful parameter for revealing bioincompatibility. The lepirudin whole blood model could be used as a rapid “screening” assay to unmask reactive surfaces, as in the case of the APA microcapsules in the present study. The presence of platelets and coagulation proteins are likely to provide a tougher environment in the whole blood model compared with, for example, the peritoneal cavity, which is a common implantation site for microspheres. Also, platelets may contribute to enhanced complement reactions [38]. However, complement and leukocytes are present in body fluids [39] and blood may come into direct contact with the capsule material during implantation, thus the same inflammatory mechanisms must be anticipated, but perhaps at lower intensities. A sensitive model like the one used in the present study is advantageous for safety evaluations, since it reveals the immune incompatibility of the implanted material in a human model.

5. Conclusion

The present study has demonstrated the effectiveness of the lepirudin-based whole blood model to reveal reactive surfaces by triggering complement and activating leukocytes. Polycation containing APA and PMCG microcapsules triggered complement and leukocyte activation, while alginate microbeads consisting of only alginate and divalent cations did not provoke complement reactions. The human whole blood model seems to be a sensitive and efficient method of revealing bioincompatibility. The method could therefore be used to determine the safety of different microcapsules for transplantation purposes.

Acknowledgements

This work has been financially supported by grants from the Chicago Diabetes Project (<http://www.chicagodiabetesproject.org/>), Norwegian Cancer Society, European Commission EP-7 **Beta Cell Therapy**, the Slovak Research and Development Agency under contract no. APVV-51-033205 and Helse-Midt **Norge**. The Chicago Diabetes Project group is also acknowledged for discussions during this work. Dorte Christiansen and Grethe Bergseth at the Department of Laboratory Medicine, Nordland Hospital, are thanked for skillful technical support.

Appendix A. Figures with essential colour discrimination

Certain figures in this article, particularly Figs. 5 and 6, are difficult to interpret in black and white. The full colour images can be found in the on-line version, at doi:doi:10.1016/j.actbio.2011.03.011.

Appendix A. Supplementary data

Supplementary data associated with this article can be found, in the online version, at doi:10.1016/j.actbio.2011.03.011.

References

644
645
646
647
648
649
650
651
652
653
654
655
656
657
658
659
660
661
662
663
664
665
666
667
668
669
670
671
672
673
674
675
676
677
678
679
680
681
682
683
684
685
686
687
688
689
690
691
692
693
694
695
696
697
698
699
700
701
702
703

[1] ~~Vos-De~~, Bucko M, Gemeiner P, Navratil M, Svitel J, Faas M, et al. Multiscale requirements for bioencapsulation in medicine and biotechnology. *Biomaterials* 2009;30:2559–70.

[2] Read TA, Stensvaag V, Vindenes H, Ulvestad E, Bjerkvig R, Thorsen F. Cells encapsulated in alginate: a potential system for delivery of recombinant proteins to malignant brain tumours. *Int J Dev Neurosci* 1999;17:653–63.

[3] Nilsson B, Korsgren O, Lambris JD, Ekdahl KN. Can cells and biomaterials in therapeutic medicine be shielded from innate immune recognition? *Trends Immunol* 2010;31:32–8.

[4] Mollnes TE, Brekke OL, Fung M, Fure H, Christiansen D, Bergseth G, et al. Essential role of the C5a receptor in E. Coli-induced oxidative burst and phagocytosis revealed by a novel lepirudin-based human whole blood model of inflammation. *Blood* 2002;100:1869–77.

[5] Andersson J, Ekdahl KN, Larsson R, Nilsson UR, Nilsson B. C3 adsorbed to a polymer surface can form an initiating alternative pathway convertase. *J Immunol* 2002;168:5786–91.

[6] Mollnes TE, Lea T, Harboe M. Detection and quantification of the terminal C5b-9 complex of human complement by a sensitive enzyme-linked immunosorbent assay. *Scand J Immunol* 1984;20:157–66.

[7] Toda M, Kitazawa T, Hirata I, Hirano Y, Iwata H. Complement activation on surfaces carrying amino groups. *Biomaterials* 2008;29:407–17.

[8] Andersson J, Ekdahl KN, Lambris JD, Nilsson B. Binding of C3 fragments on top of adsorbed plasma proteins during complement activation on a model biomaterial surface. *Biomaterials* 2005;26:1477–85.

[9] Arima Y, Kawagoe M, Furuta M, Toda M, Iwata H. Effect of swelling of poly(vinyl alcohol) layers on complement activation. *Biomaterials* 2010;31:6926–33.

[10] Qi M, Strand BL, Morch Y, Lacik I, Wang Y, Salehi P, et al. Encapsulation of human islets in novel inhomogeneous alginate-Ca²⁺/Ba²⁺ microbeads: in vitro and in vivo function. *Artif Cells Blood Substit Immobil Biotechnol* 2008;36:403–20.

[11] Qi M, Morch Y, Lacik I, Formo K, Marchese E, Wang Y, Wang S, et al. Prolonged immunosuppression-free survival of human islets inhomogeneous Ca²⁺/Ba²⁺-alginate microbeads in diabetic immunocompetent mice. Unpublished work.

[12] Wang T, Lacik I, Brissova M, Anilkumar AV, Prokop A, Hunkeler D, et al. An encapsulation system for the immunoisolation of pancreatic islets. *Nat Biotechnol* 1997;15:358–62.

[13] Wang T, Adcock J, Kuhlreiter W, Qiang D, Salleng KJ, Trenary I, et al. Successful allotransplantation of encapsulated islets in pancreatized canines for diabetic management without the use of immunosuppression. *Transplantation* 2008;85:331–7.

[14] Lacik I, Brissova M, Anilkumar AV, Powers AC, Wang T. New capsule with tailored properties for the encapsulation of living cells. *J Biomed Mater Res* 1998;39:52–60.

[15] King A, Sandler S, Andersson A. The effect of host factors and capsule composition on the cellular overgrowth on implanted alginate capsules. *J Biomed Mater Res* 2001;57:374–83.

[16] King A, Strand B, Rokstad AM, Kulseng B, Andersson A, Skjak-Braek G, et al. Improvement of the biocompatibility of alginate/poly-L-lysine/alginate microcapsules by the use of epimerized alginate as a coating. *J Biomed Mater Res A* 2003;64:533–9.

[17] Strand BL, Ryan TL, In't VP, Kulseng B, Rokstad AM, Skjak-Brek G, et al. Poly-L-lysine induces fibrosis on alginate microcapsules via the induction of cytokines. *Cell Transplant* 2001;10:263–75.

[18] Safley SA, Cui H, Cauffiel S, Tucker-Burden C, Weber CJ. Biocompatibility and immune acceptance of adult porcine islets transplanted intraperitoneally in diabetic NOD mice in calcium alginate poly-L-lysine microcapsules versus barium alginate microcapsules without poly-L-lysine. *J Diabetes Sci Technol* 2008;2:760–7.

[19] Mollnes TE, Redl H, Hogasen K, Bengtsson A, Garred P, Speilberg L, et al. Complement activation in septic baboons detected by neopeptide-specific assays for C3b/iC3b/C3c, C5a and the terminal C5b-9 complement complex (TCC). *Clin Exp Immunol* 1993;91:295–300.

[20] Strand BL, Morch YA, Espevik T, Skjak-Braek G. Visualization of alginate-poly-L-lysine-alginate microcapsules by confocal laser scanning microscopy. *Biotechnol Bioeng* 2003;82:386–94.

[21] De Vos P, De Haan BJ, Wolters GH, Strubbe JH, van Schilfgaarde R. Improved biocompatibility but limited graft survival after purification of alginate for microencapsulation of pancreatic islets. *Diabetologia* 1997;40:262–70.

[22] Anilkumar AV, Lacik I, Wang TG. A novel reactor for making uniform capsules. *Biotechnol Bioeng* 2001;75:581–9.

[23] Lappegard KT, Fung M, Bergseth G, Riesenfeld J, Lambris JD, Videm V, et al. Effect of complement inhibition and heparin coating on artificial surface-induced leukocyte and platelet activation. *Ann Thorac Surg* 2004;77:932–41.

[24] Morch YA, Donati I, Strand BL, Skjak-Braek G. Effect of Ca²⁺, Ba²⁺, and Sr²⁺ on alginate microbeads. *Biomacromolecules* 2006;7:1471–80.

[25] Gros P, Milder FJ, Janssen BJ. Complement driven by conformational changes. *Nat Rev Immunol* 2008;8:48–58.

[26] Tam SK, Dusseault J, Polizu S, Menard M, Halle JP, Yahia L. Physicochemical model of alginate-poly-L-lysine microcapsules defined at the micrometric/nanometric scale using ATR-FTIR, XPS, and ToF-SIMS. *Biomaterials* 2005;26:6950–61.

[27] McNally AK, Anderson JM. Complement C3 participation in monocyte adhesion to different surfaces. *Proc Natl Acad Sci USA* 1994;91:10119–23.

[28] Wright SD, Weitz JI, Huang AJ, Levin SM, Silverstein SC, Loike JD. Complement receptor type three (CD11b/CD18) of human polymorphonuclear leukocytes recognizes fibrinogen. *Proc Natl Acad Sci USA* 1988;85:7734–8.

[29] Rinder CS, Smith MJ, Rinder HM, Cortright DN, Brodbeck RM, Krause JE, et al. Leukocyte effects of C5a-receptor blockade during simulated extracorporeal circulation. *Ann Thorac Surg* 2007;83:146–52.

[30] Schwartz-Albiez R, Adams Y, Von der Lieth CW, Mischnick P, Andrews KT, Kirschfink M. Regioselectively modified sulfated cellulose as prospective drug for treatment of malaria tropica. *Glycoconj J* 2007;24:57–65.

[31] Eisen V, Loveday C. Effect of cellulose sulphate on serum complement. *Br J Pharmacol* 1970;39:831–3.

[32] Eisen V, Loveday C. In vivo effects of cellulose sulphate on plasma kininogen, complement and inflammation. *Br J Pharmacol* 1971;42:383–91.

[33] Toso C, Mathe Z, Morel P, Oberholzer J, Bosco D, Sainz-Vidal D, et al. Effect of microcapsule composition and short-term immunosuppression on intraportal biocompatibility. *Cell Transplant* 2005;14:159–67.

[34] De Vos P, De Haan B, van Schilfgaarde R. Effect of the alginate composition on the biocompatibility of alginate-polylysine microcapsules. *Biomaterials* 1997;18:273–8.

[35] Lappegard KT, Fung M, Bergseth G, Riesenfeld J, Mollnes TE. Artificial surface-induced cytokine synthesis: effect of heparin coating and complement inhibition. *Ann Thorac Surg* 2004;78:38–44.

[36] Lappegard KT, Bergseth G, Riesenfeld J, Pharo A, Magotti P, Lambris JD, et al. The artificial surface-induced whole blood inflammatory reaction revealed by increases in a series of chemokines and growth factors is largely complement dependent. *J Biomed Mater Res A* 2008;87:129–35.

[37] Lappegard KT, Christiansen D, Pharo A, Thorgersen EB, Hellerud BC, Lindstad J, et al. Human genetic deficiencies reveal the roles of complement in the inflammatory network: lessons from nature. *Proc Natl Acad Sci USA* 2009;106:15861–6.

[38] Markiewski MM, Nilsson B, Ekdahl KN, Mollnes TE, Lambris JD. Complement and coagulation: strangers or partners in crime? *Trends Immunol* 2007;28:184–92.

[39] Akalin HE, Fisher KA, Laleli Y, Caglar S. Bactericidal activity of ascitic fluid in patients with nephrotic syndrome. *Eur J Clin Invest* 1985;15:138–40.

704
705
706
707
708
709
710
711
712
713
714
715
716
717
718
719
720
721
722
723
724
725
726
727
728
729
730
731
732
733
734
735
736
737
738
739
740
741
742
743
744
745
746
747
748
749
750
751
752
753
754
755
756
757
758
759
760
761
762
763
764
765